ELSEVIER

Signal Processing 70 (1998) 23–42

SIGNAL PROCESSING

Suppression of moiré patterns in scanned halftone images[1]

James Chingyu Yang[2], Wen-Hsiang Tsai*

Department of Computer and Information Science, National Chiao Tung University, 1001 Ta Hsueh Road, Hsinchu, Taiwan 300, People's Republic of China

Received 18 January 1996; received in revised form 6 July 1998

Abstract

Moiré patterns often appear in the image obtained from scanning an image printed on a magazine or a newspaper. The patterns do not exist in the original printing but come from alias sampling of screened halftone pictures. A strategy to design a moiré suppression scanning procedure is proposed. Fourier analysis is presented for both the screening and the scanning processes, from which a formula is derived to calculate a special scanning resolution, called moiré controlling scanning resolution. With the moiré scanning resolution, an input halftone image is scanned and the moiré signals can be confined in programmed frequency areas. After filtering out the signals in those areas, the original can be restored. Some useful spatial filters for this purpose are designed. Experimental results are shown to demonstrate the feasibility of the proposed approach.

Zusammenfassung

Beim Scannen eines Zeitungs- oder Zeitschriftenbildes treten oft Moiré-Muster auf. Diese Muster existieren nicht im Original, sondern entstehen durch überlappende Abtastung von Halbtonbildern. Vorgeschlagen wird eine Strategie zum Entwurf eines Abtastverfahrens mit Moiré-Unterdrückung. Eine Fourieranalyse sowohl für die Rasterungs- als auch für die Abtastungsprozesse wird vorgestellt, aus der eine Formel zur Berechnung einer speziellen Abtastauflösung hergeleitet wird, die Moiré-kontrollierende Abtastauflösung genannt wird. Mit dieser Auflösung wird ein Halbtonbild gescannt und die Moiré-Signale können auf einen programmierten Frequenzbereich beschränkt werden. Nach dem Herausfiltern dieser Signale aus eben diesen Frequenzbereichen kann das Original wiederhergestellt werden. Zu diesem Zweck werden einige nützliche räumliche Filter entworfen. Experimentelle Ergebnisse werden gezeigt, um die Durchführbarkeit des vorgeschlagenen Vorgehensweise zu demonstrieren.

Résumé

Des motifs de moiré apparaissent souvent dans des images obtenues par numérisation d'images imprimées dans un magazine ou un journal. Ces motifs n'existent pas dans l'impression originale mais proviennent du repli de spectre des images en demi-teintes affichées. Nous présentons ici une stratégie de conception d'une procédure de numérisation supprimant ce moiré. Une analyse de Fourier est présentée à la fois pour l'affichage et pour la numérisation, dans laquelle

* Corresponding author. Tel.: 035 715 900; fax: 035 721 490.

[1] This work was supported partially by National Science Council, Republic of China under grant NSC85-2221-E009-011.

[2] Also with Tungnan Junior College of Technology.

0165-1684/98/$ – see front matter
PII: S0165-1684(98)00111-X

une formule est dérivée afin de calculer une résolution de numérisation spéciale, appelée "résolution de numérisation pour le contrôle du moiré". Avec une telle résolution, une image en demi-teintes est numérisée et les signaux de moiré peuvent être confinés dans une plage de fréquences programmée. Aprés filtrage des signaux dans cette plage, l'image originale peut être restaurée. Des filtres spatiaux ont été conçus dans ce but. Des résultats expérimentaux sont présentés, pour démontrer la faisabilité de cette approche.

Keywords: Moiré controlling scanning resolution; Moiré pattern; Halftone image; Printing; Scanning; Fourier analysis; Spatial filter; Image restoration; Moiré suppression

1. Introduction

Most printed images are produced as bi-level images [11]. And halftone screening is employed to convert a continuous-tone image into a halftoned one which consists of numerous tiny screening dots. The size of each dot varies according to the various tones of the original image. Halftoning systems rely on human vision that integrates numerous small features to achieve an illusion of the original continuous-tone image. The dots in the halftone image are spread periodically. They are also arranged orthogonally to comfort human eyes. A raster image processor (RIP) is required to generate the halftone images for digital reproduction. A sample continuous-tone image and a halftone image generated from it are shown in Fig. 1.

When we scan an image with periodic structures or superpose multiple color screens, aliasing is unavoidable and additional moiré patterns will usually appear in the scanning or superposition result [3,6,8]. Because screen dots are repeated periodically in a halftone image, scanning a halftone image will generate additional moiré patterns. Fourier analysis can be employed to describe this phenomenon. Some researches [1,5] described the aliasing phenomenon for the screening process. In this paper, Fourier analyses of both the modern digital screening and the scanning processes will be presented.

According to the functionality of scanner hardware, the image scanning process can be divided into three major stages. The first stage is pre-filtering which is an optical process related to the characteristics of the scanner lens. Using a large drum

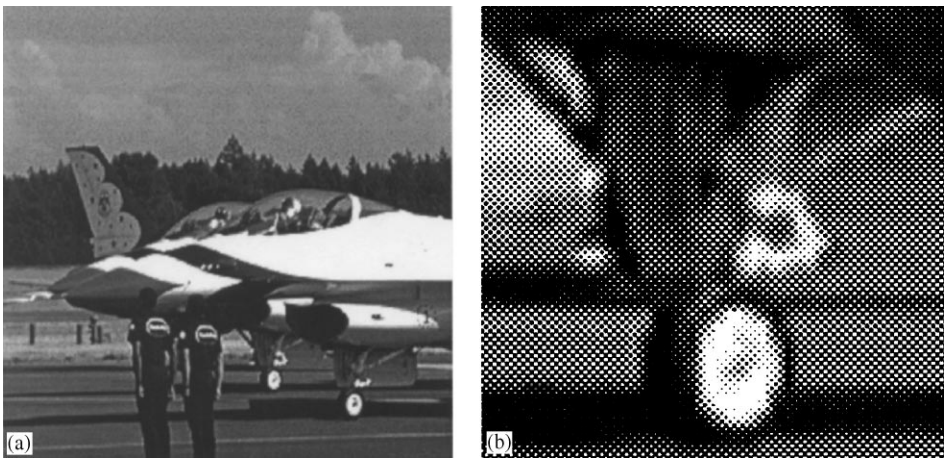

Fig. 1. A halftone image creates an illusion of a continuous tone image. (a) The original continuous tone image. (b) Part of the generated halftone image.

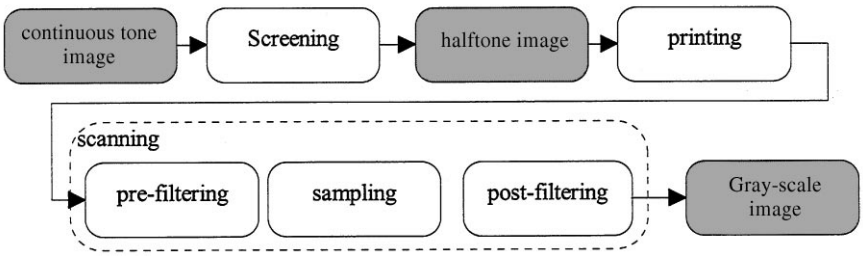

Fig. 2. The screening and scanning process.

scanner, a user can adjust the focus and the apertures of the lens to make the scanning result sharper or smoother. The next stage is sampling that is realized by a motor moving or a CCD arrangement. A user can adjust the scanning resolution to change the spacing of the sampling grid. The brightness values of the scanned picture are quantized into digital values. The final stage is post-filtering which is a software process employed to correct digital image values by gamma correction, look up tables, or other filters.

Fig. 2 shows a flowchart of the screening and the scanning processes. For gray-scale images, the moiré phenomenon mainly comes from sampling the screen of printing result in the scanning step. Some works proposed to suppress moiré patterns are reviewed in the following.

Smoothing is a natural way to remove high-frequency noise. A scanner operator usually adjusts the focus or the aperture in the pre-filtering stage to smooth the scanning result in order to suppress the moiré patterns. As is well known, smoothing is a low-pass filter in the frequency domain [8], which reduces the high-frequency halftone screen signals. It removes most periodic structures of the image. There are however problems that are related to smoothing. First, the image will be blurred. Next, it is difficult to perform good aperture or focus adjustment. Only high-end drum scanners support these kinds of adjustments in the pre-filtering stage.

Using inverse halftoning as a post-filter to remove moiré patterns has also been tried [2,4]. First, the details of the halftone image are scanned with very high resolution. By analysis of each screen dot, it is possible to derive a corresponding gray-scale image. However, much processing time may be required, and high-resolution scanning takes longer time and larger memory space.

In Shu and Yeh [10], possible factors that cause moiré patterns were analyzed. A rule was figured out to formulate the relationship between scanning resolution, screening resolution, their angles, and moiré visibility. A suggestion to select a scanning resolution was proposed for scanning to yield minimum visibility of moiré patterns.

Russ [9] removed periodic information of images in the frequency domain by manual masking operations. However, it is in general difficult to determine in the frequency domain the spots that cause moiré patterns in the original image.

Roetling [7] proposed a halftoning method with moiré suppression which can be used for the reproduction of halftone images. Using an adaptive thresholding process, the average value of each halftone cell on the reproduced halftone result can be kept identical to the average value of the source halftone image, and the moiré patterns on the high resolution halftone output can then be suppressed. This moiré suppression method keeps the screen structures of the source halftone image, however, this is not necessary for the ordinary gray scale image representation.

A new strategy is proposed in the present paper to design a moiré suppression procedure for halftone image scanning. After the screening angle and frequency are measured by a digital screen tester. We derive a formula for a moiré controlling scanning resolution (MCSR). Using the derived resolution, the scanning confines the positions of the moiré signals in some frequency areas. Signals in those areas are then suppressed by some spatial filters designed in this study.

In the remainder of this paper, we formulate the screening and scanning processes in Section 2. Using Fourier analysis, we point out how moiré patterns are generated by halftone image scanning. In Section 3, we describe the proposed moiré suppression strategy and the proposed digital screen tester. Some experimental results are shown in Section 4, followed by conclusions in Section 5.

2. Fourier analyses of moiré phenomenon

2.1. Fourier analysis of screening

The halftoning process is accomplished by a dynamic thresholding operation based on a thresholding function. The thresholding process can be modeled by the following formula:

$$\mathrm{h}(\boldsymbol{r}) = g(\boldsymbol{r}) \perp s(\boldsymbol{r}) = \begin{cases} 1, & \text{if } g(\boldsymbol{r}) \geqslant s(\boldsymbol{r}), \\ 0, & \text{if } g(\boldsymbol{r}) < s(\boldsymbol{r}), \end{cases} \tag{1}$$

where $\perp$ denotes the thresholding operator, the vector $\boldsymbol{r}$ specifies a position in the spatial domain, the function $g(\boldsymbol{r})$ defines the intensity of the source continuous-tone image with range [0,1], $s(\boldsymbol{r})$ is the thresholding function, and the function $h(\boldsymbol{r})$ defines the signals on the *output halftone image*. Here, we use intensity value 0 to represent black and 1 to represent white. Since a halftone image is bi-level, the value of the function for each pixel is either 0 or 1. Fig. 3 illustrates the conversion of a source continuous-tone image into a halftone image.

The thresholding function $s(\boldsymbol{r})$, called *screening function*, can be programmed to generate different halftone patterns. As discussed before, the patterns are created to generate a simulated illusion of the original continuous-tone image. Normally, an array of varying-sized black *screen dots* is generated. Ideally, the screen dots are very small and can hardly be detected by human eyes. They are distributed uniformly and orthogonally to create a stable illusion. We can use the following convolution formula to model the screening function $s(\boldsymbol{r})$:

$$s(\boldsymbol{r}) = s_d(\boldsymbol{r}) * \xi_s(\boldsymbol{r}), \tag{2}$$

where $s_d(\boldsymbol{r})$ specifies the *screening dot function* and $\xi_s(\boldsymbol{r})$ specifies the *screening grid*. The screening dot function defines the shape of the dot. Normally, it is a symmetric and homogeneous decreasing function. Some frequently used screening dot functions have round, elliptical, diamond or square shapes. Occasionally, people use stochastic screening functions for low-resolution printers; in the present contribution, however, we only deal with periodic screening functions. The screening grid can be established by two orthogonal bases, $\boldsymbol{r}_{s1}$ and $\boldsymbol{r}_{s2}$, defined below:

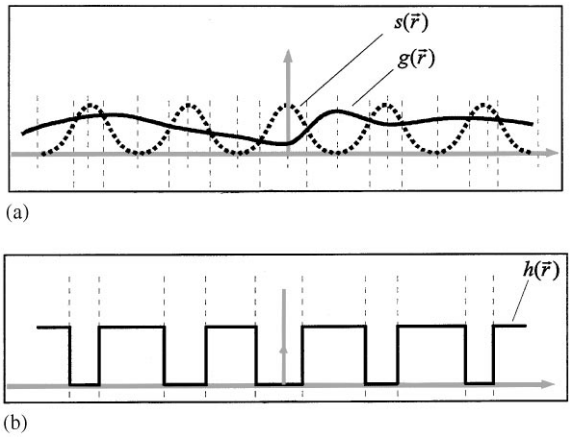

Fig. 3. The dynamic thresholding operation of the screening process. (a) The source intensity function (solid) and the screening function (dashed). (b) The output halftone intensity function.

$$\xi_s(\boldsymbol{r}) = \sum_{m=-\infty}^{\infty} \sum_{n=-\infty}^{\infty} \delta(\boldsymbol{r} - m\boldsymbol{r}_{s1} - n\boldsymbol{r}_{s2}). \tag{3}$$

Convolution of the screening grid with the screening dot function distributes the screening dot function uniformly and orthogonally on the screening space. Obviously, the screening dot function is confined in a square or parallelogram range framed by each screening grid. The screen dot function is to be designed so as to avoid any overlapping caused by convolution. Fig. 4 shows the effective area of the screening dot function for the central dot.

In the following analysis, we formulate the digital screening process, in order to show some properties of the screened halftone images.

In a source digital gray-scale image, each pixel has a certain quantized gray value. Several

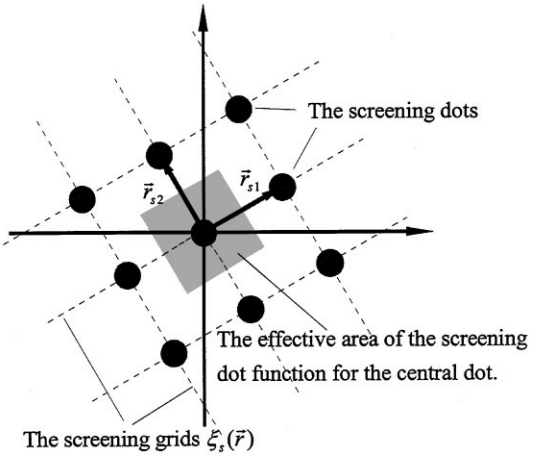

Fig. 4. The screening grids and the effective area for the screening dot function.

non-overlapping *image plates* can be generated from the source digital gray-scale image according to the gray values. All the pixels on an identical image plate have equivalent gray values. For example, on image plate $g_m(\boldsymbol{r})$, pixels with gray value m retain their values and the remaining pixels are cleared to 0, i.e.,

$$g_m(\boldsymbol{r}) = \begin{cases} m, & \text{if } g(\boldsymbol{r}) = m, \\ 0, & \text{elsewhere.} \end{cases} \tag{4}$$

For example, a four-colored digital multi-intensity image, as shown in Fig. 5(a), can be separated into four individual image plates $g_0(\boldsymbol{r})$, $g_1(\boldsymbol{r})$, $g_2(\boldsymbol{r})$ and $g_3(\boldsymbol{r})$ as shown in Fig. 5(b). If we perform a screening process on each image plate $g_m(\boldsymbol{r})$, it is easy to see that the resulting halftone image $g_m(\boldsymbol{r}) \perp s(\boldsymbol{r})$, called *component halftone image plate*, will keep the non-overlapping property. Adding these component halftone image plates, a screened halftone image is generated which is equivalent to the one that is generated directly from the source image by the thresholding process with the same screening function $s(\boldsymbol{r})$. Accordingly, we can define the output halftone image as follows:

$$h(\boldsymbol{r}) = g(\boldsymbol{r}) \perp s(\boldsymbol{r}) = \sum_{m=0}^{N-1} [g_m(\boldsymbol{r}) \perp s(\boldsymbol{r})]. \tag{5}$$

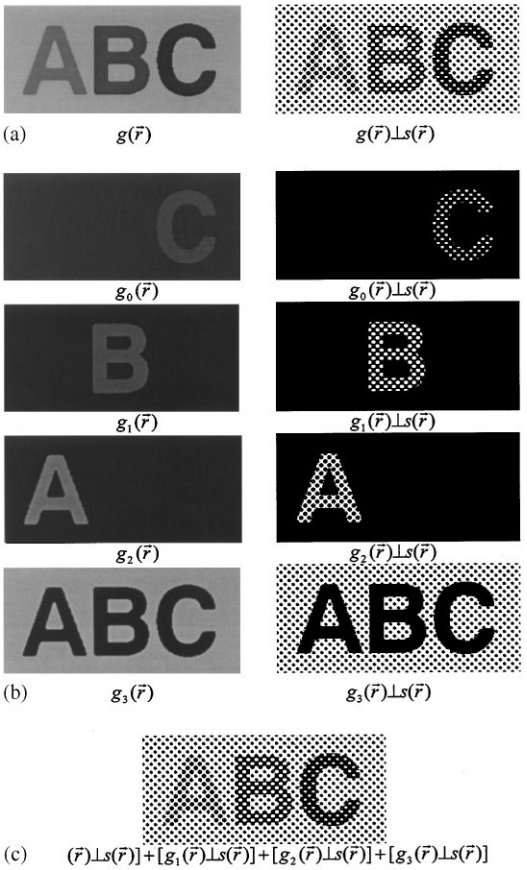

Fig. 5. The screened halftone image is idential to the summation of all the screened halftone images of the component image plates of the source image. (a) The source gray-scaled image and the corresponding screened halftone image. (b) Four component image plates (left) obtained from the source image and their corresponding screened halftone images. (c) Adding all the screened halftone image of each component image plates in (b) yields the same screened halftone image as the right image in (a).

Because each pixel value of $g_m(\boldsymbol{r})$ is either 0 or m, the thresholding process of $g_m(\boldsymbol{r}) \perp s(\boldsymbol{r})$ only alters those pixels with gray value m. All the pixels having gray values different to m must be 0, and are not altered by the thresholding operation. In other words, we can regard the image plate as an image mask which clears those pixels on a *constant screen plate* to 0 wherever the corresponding pixels on the mask have gray value 0. Here, the constant screen

plate has uniform screen dots and is defined as follows:

$$s_m(\boldsymbol{r}) = m \perp s(\boldsymbol{r}). \tag{6}$$

Normally people use the logical AND operation to describe the mask operation. Because images $(1/m)g_m(\boldsymbol{r})$ and $m \perp s(\boldsymbol{r})$ are binary with intensity values either 0 or 1, we can also use multiplication to model the masking operation mathematically. That is, the thresholding operation of the image plate $g_m(\boldsymbol{r})$ can also be written as

$$g_m(\boldsymbol{r}) \perp s(r) = \left[\frac{1}{m} g_m(\boldsymbol{r}) m\right] \perp s(\boldsymbol{r}) = \frac{1}{m} g_m(\boldsymbol{r}) s_m(\boldsymbol{r}). \tag{7}$$

And the halftone image $h(\boldsymbol{r})$ in Eq. (5) can be modified as

$$h(\boldsymbol{r}) = \sum_{m=0}^{N-1} \frac{1}{m} g_m(\boldsymbol{r}) s_m(\boldsymbol{r}). \tag{8}$$

By comparing Eqs. (1) and (8), we see that the thresholding operator does not appear explicitly. It is now possible to analyze the Fourier transform of the output halftone image. The Fourier transform of Eq. (8) is

$$H(\boldsymbol{w}) = \sum_{m=0}^{N-1} \left(\frac{1}{m} G_m(\boldsymbol{w}) * S_m(w)\right), \tag{9}$$

where $G_m(\boldsymbol{w})$ is the Fourier transform of image plate $g_m(\boldsymbol{r})$, and $S_m(\boldsymbol{w})$ is the Fourier transform of constant screen plate $s_m(\boldsymbol{r})$.

The constant screen plates $s_m(\boldsymbol{r})$ in Eq. (6) are an output of a thresholding process, i.e., a binary images that contains pixels with gray values either 0 or 1. As described before, the thresholding function $s(\boldsymbol{r})$ in Eq. (2) is established by duplicating the screening dot function $s_d(\boldsymbol{r})$ on the screening grid. The effective areas of the screening dot functions do not overlap. When thresholding a constant, an identical screen dot pattern will be generated in each effective area. In other words, the result of the thresholding is an array of screen dots, which is spread on the screening grid. Hence, the constant screen plates can be formulated as a convolution of the screening grid and the screened dot that is generated by the thresholding operation $m \perp s_d(\boldsymbol{r})$. Therefore, the constant screen plates can be formulated as

$$s_m(\boldsymbol{r}) = [m \perp s_d(\boldsymbol{r}]) * \xi_s(\boldsymbol{r}),$$

where $\xi_s(\boldsymbol{r})$ is described by Eq. (3). And the Fourier transform of the above equation is

$$s_m(w) = \Im[m \perp s_d(r)\} \Xi_s(\boldsymbol{w}), \tag{10}$$

where $\Xi_s(\boldsymbol{w})$ is the *reciprocal screening grid* in the frequency domain defined as

$$\Xi_s(\boldsymbol{w}) = C_1 \sum_{m=-\infty}^{\infty} \sum_{n=-\infty}^{\infty} \delta(\boldsymbol{w} - m\boldsymbol{w}_{s1} - n\boldsymbol{w}_{s2}), \tag{11}$$

where C_1 is a constant; and $\boldsymbol{w}_{s1}$ and $\boldsymbol{w}_{s2}$ are the reciprocals of the screening bases, $\boldsymbol{r}_{s1}$ and $\boldsymbol{r}_{s2}$, respectively. Obviously, non-zero terms only exist at the nodes of the screening grid in the frequency domain. Fig. 6 shows an example of the constant screen plate in the spatial and the frequency domains.

Because the screening structure is used to create the illusion of a gray-scale image, the screen dots must be small enough to make the detail of the source image distinguishable, i.e., the screening signal should have much higher frequency than that of the image plate. The signals in the image plate $G_m(\boldsymbol{w})$ should vanish outside the rectangle with the boundary of $\pm\frac{1}{2}\boldsymbol{w}_{s1}$ and $\pm\frac{1}{2}\boldsymbol{w}_{s2}$. Convolution of $G_m(\boldsymbol{w})$ and the Fourier transform of the constant screen plate $S_m(\boldsymbol{w})$ in Eq. (9) creates significant signal components at the nodes of the reciprocal screening grid in the frequency domain. Fig. 7 shows the result of such a convolution for the one-dimensional case, in which the signals of the

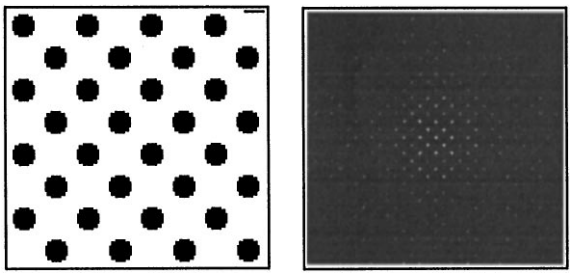

Fig. 6. An example of the constant screen plate (left) and its corresponding Fourier spectrum (right).

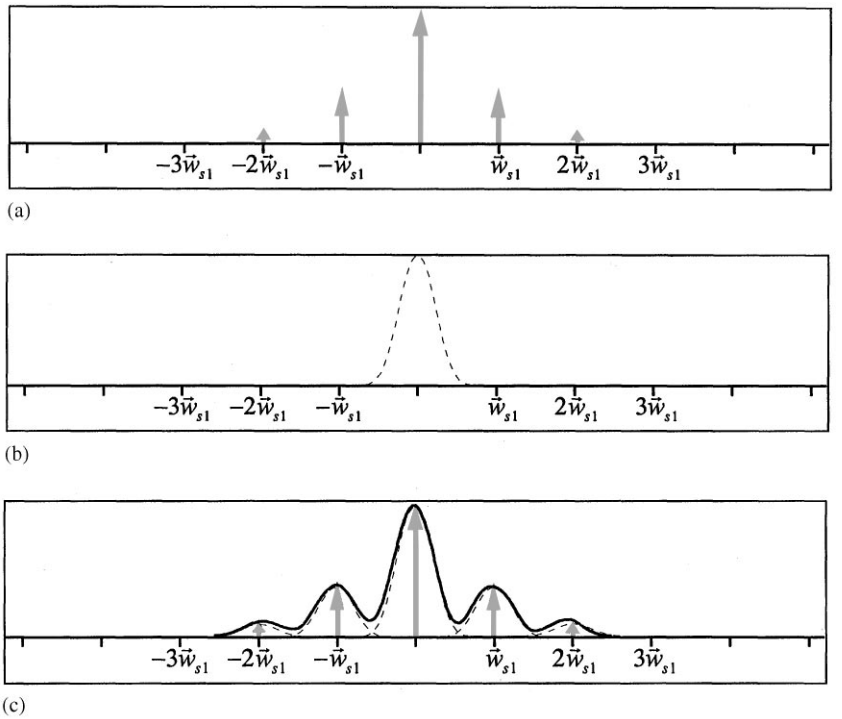

Fig. 7. The result of the convolution of $G_m(\boldsymbol{w})$ and $S_m(\boldsymbol{w})$. (a) The constant screen plate $S_m(\boldsymbol{w})$ in the frequency domain. (b) The signal of component image plate $G_m(\boldsymbol{w})$ in the frequency domain. (c) The result of the convolution of (a) and (b).

image plate are shown as a dashed line and the result of the convolution is shown as a solid line. Here, we call each significant signal component as a *screen signal component* (SSC). The screen signal components can be classified by frequency. We denote by SSC_α the set of screen signal components placed within a circle with radius α in the frequency domain. Fig. 8 shows the result of the convolution and the screen signal components of various radii in the frequency domain.

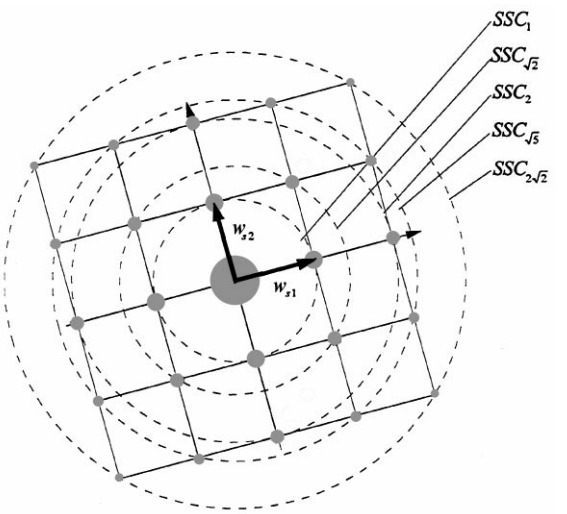

Fig. 8. The screen signal components.

2.2. Fourier analysis of scanning

As described before, there are three stages in the scanning process. We use the following equation to model the first two stages of scanning, namely, pre-filtering and sampling:

$$g'(\boldsymbol{r}) = [h(\boldsymbol{r}) * a(\boldsymbol{r})] \times \xi_n(\boldsymbol{r}), \tag{12}$$

where $a(\boldsymbol{r})$ is the *aperture function* which defines the aperture transmittance of the scanner lens; $h(\boldsymbol{r})$ is the source halftone image produced by the RIP and printed on paper; $g'(\boldsymbol{r})$ is the gray-scale image resulting from scanning; and $\xi_n(\boldsymbol{r})$ denotes the scanning grid defined as

$$\xi_n(\boldsymbol{r}) = \sum_{m=-\infty}^{\infty} \sum_{n=-\infty}^{\infty} \delta(\boldsymbol{r} - m\boldsymbol{\alpha}_1 - n\boldsymbol{\alpha}2), \tag{13}$$

where $\boldsymbol{\alpha}_1$ and $\boldsymbol{\alpha}_2$ are the basis vectors of the scanning grid; and m and n are integers.

The first part in the right hand side of Eq. (12), the convolution $h(\boldsymbol{r}) * a(\boldsymbol{r})$, models the pre-filtering step of the scanning process, in which light is reflected from the printed halftone image and collected by the optics structure of the scanner. After that, light is sampled at positions $m\boldsymbol{\alpha}_1 + n\boldsymbol{\alpha}_2$ in the sampling step. The aperture function is a gaussian function. The larger the distance from the sampling point, the less the light can be transmitted. The Fourier transform of Eq. (12) is

$$G(\boldsymbol{w}) = [H(\boldsymbol{w}) \times A(\boldsymbol{w})] * \Xi_n(\boldsymbol{w}), \tag{14}$$

where $H(\boldsymbol{w})$ is the Fourier transform of $h(\boldsymbol{r})$, $A(\boldsymbol{w})$ is the Fourier transform of $a(\boldsymbol{r})$, and $\Xi_n(\boldsymbol{w})$ denotes the reciprocal scanning grid defined as

$$\Xi_n(\boldsymbol{w}) = C_2 \sum_{k=-\infty}^{\infty} \sum_{l=-\infty}^{\infty} \delta(\boldsymbol{w} - k\boldsymbol{u}_1 - l\boldsymbol{u}_2), \tag{15}$$

where $\boldsymbol{u}_1$ and $\boldsymbol{u}_2$ are the reciprocal basis derived from $\boldsymbol{\alpha}_1$ and $\boldsymbol{\alpha}_2$; k and l are integers; and C_2 is a constant.

The first part of the right hand side of Eq. (14), i.e., the product $H(\boldsymbol{w}) \times A(\boldsymbol{w})$ of the aperture function and the original halftone image in the frequency domain, is shown in Fig. 9 for the one-dimensional case. According to the previous discussion, the halftone image $H(\boldsymbol{w})$ has signal components at frequencies $m\boldsymbol{w}_1 + n\boldsymbol{w}_2$. The product $H(\boldsymbol{w}) \times A(\boldsymbol{w})$ should also have corresponding signal components at these positions.

Then, the product is convolved with the grid spread by basis vectors $\boldsymbol{u}_1$ and $\boldsymbol{u}_2$. By the convolution, the signal components of $H(\boldsymbol{w}) \times A(\boldsymbol{w})$ centered at $m\boldsymbol{w}_1 + n\boldsymbol{w}_2$ are reproduced at each node of the scanning grid. An illustration of the result of such convolution for the 2-dimensional case is shown in Fig. 10 in which some screen signal components are shifted into the low-frequency area (the shaded square area). These low-frequencies screen signal components introduce additional moiré patterns. Let us define *moiré signal set* $\mathrm{MSS}_{\alpha,\beta}$ as the set of the shifted screen signal components in the low frequency area which originally are in SSC_α and are

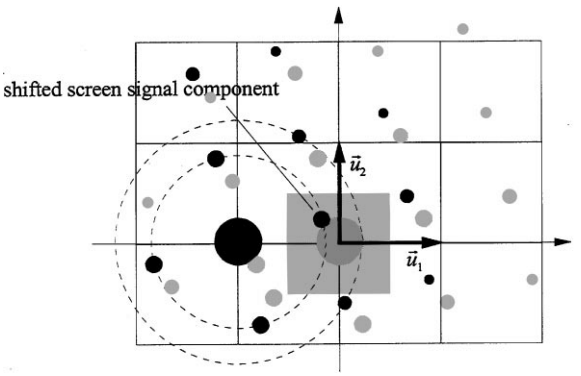

Fig. 10. Moiré signals are generated by any screen signal components shifted into the low frequency area (one of the cases is shown).

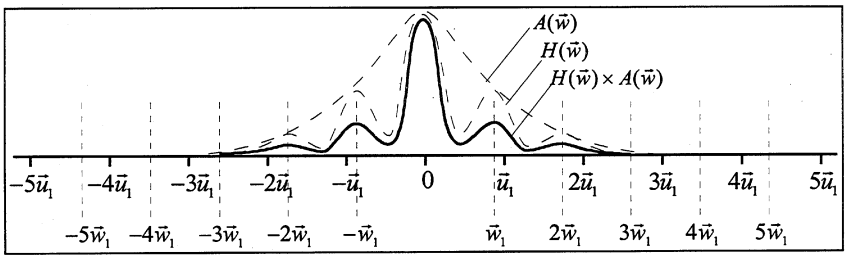

Fig. 9. $H(\boldsymbol{w}) \times A(\boldsymbol{w})$ in the frequency domain.

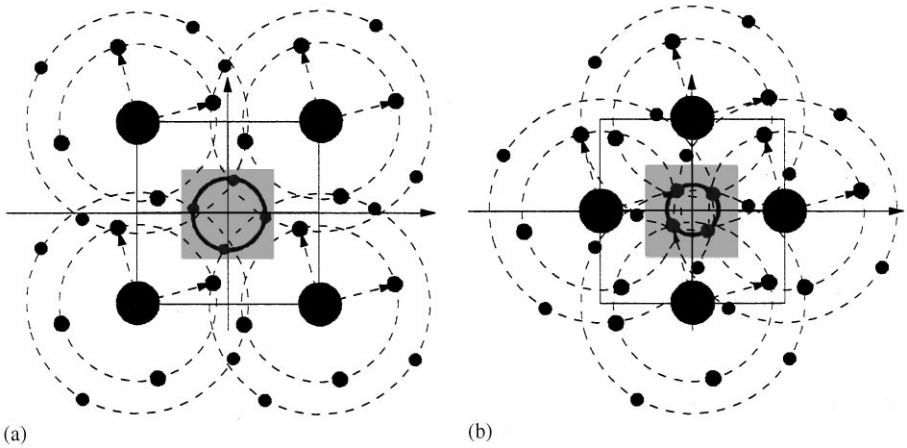

Fig. 11. Moiré signals sets. (a) $MSS_{\sqrt{2},\sqrt{2}}$. (b) $MSS_{1,1}$.

shifted due to convolution with the impulses on the reciprocal scanning grid $\Xi_n(\boldsymbol{w})$ with $|\boldsymbol{w}| = \beta$. Fig. 11 shows two examples of moiré signal sets $MSS_{\sqrt{2},\sqrt{2}}$ and $MSS_{1,1}$.

The scanning resolution, the screen frequency and the screen angle are parameters that may alter the positions of the moiré signal sets in the frequency domain. For commercial reproduction, the screening resolution is normally 100 to 200 LPI and the screening angle is often fixed to 0° (90°), 15° (105°), 45° (135°) and 75° (165°). For black and white printing, the 45° screening angle is the most comfortable screening angle for human eyes. The scanning resolution varies for different applications. Resolutions between 100 DPI to 600 DPI are normally selected. Before scanning, the screen frequency and the screen angle of the source halftone image can be measured by a screen tester. The angle of the scanning grid is fixed by scanner hardware. If we want to alter the moiré patterns that appear on the scanned image, changing the scanning resolution becomes the only way.

3. Proposed moiré suppression method

Moiré patterns can be altered by adjusting the scanning resolution. In this section, we will show that a specific scanning resolution, called "moiré controlling scanning resolution" (MCSR), can be derived from certain given screen angles and screen frequencies, and by using the MCSR, the moiré signals of a halftone image can be confined in programmed areas. We will also show that band-pass filters can be employed to suppress the signals in these confining areas and a better image can be obtained. Each band-pass filtering operation is accomplished by the use of a combination of some spatial filters. Some useful spatial filters are designed in this study and shown in this section. Fourier transforms are not performed and the filtering speed is fast. Screen parameters, including the screen angle and the screen frequency, are required for the calculation of the desired MCSR. We also propose a digital screen tester to measure the screen parameters precisely.

3.1. Moiré controlling scanning resolution

The MCSR is a value that can be calculated by two parameters, the screen frequency and the screen angle, of the source halftone image. In order to describe the MCSR, three cases, which cover all possible conditions of source halftone images, are checked.

The first case occurs when the screen angle is 0° (or 90°). This situation is shown in Fig. 12(a). If we select the scanning resolution defined in Eq. (16)

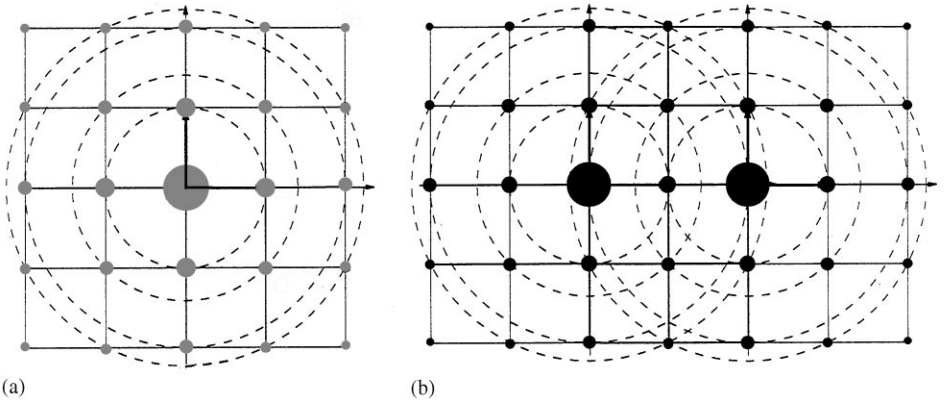

Fig. 12. Screen signal components (MCSR) of 0° screen. (a) The SSC of 0° halftone. (b) The SSC of 0° halftone on the image scanned by MCSR(0°) using $n = 1$.

below to scan such an image, all the moiré signal sets will perfectly overlap at the nodes of the screening grid so that the screen signal components are enhanced and no additional moiré patterns are generated:

$$\mathrm{MCSR}(0^\circ) = n \times f_{\mathrm{screen}}, \tag{16}$$

where MCSR(0°) denotes the MCSR for 0° (or 90°); f_{screen} is the screen frequency; and n is an integer number. This situation is shown in Fig. 12(b).

The next case occurs when the screen angle is 45°. As we know, the angle of 45° is the most frequently used halftone angle for black and white image reproduction. By using the MCSR for 45° calculated by Eq. (17) below, the screen signal components also perfectly overlap on the screening grid:

$$\mathrm{MCSR}(45^\circ) = n \times f_{\mathrm{screen}} \times \frac{1}{\sqrt{2}}, \tag{17}$$

where MCSR(45°) denotes the MCSR for 45°; f_{screen} is the screen frequency; and n is an integer number. This situation is shown in Fig. 13. For example, for a 45° screened halftone image with the screen frequency of 150 LPI, the MCSR is, by Eq. (17) using $n = 3$, calculated to be 318 DPI.

The third case occurs when the screen angle is not 0°, 90° or 45°. The positions of the screen signal components are altered if the screen angle is changed. For this case, we generalize the MCSR calculated by Eq. (16) or Eq. (17) to be Eq. (18) as follows:

$$\mathrm{MCSR}(\theta) = n \times f_{\mathrm{screen}} \times \cos\theta, \tag{18}$$

where MCSR(θ) denotes the MCSR of any angle θ; f_{screen} is the screen frequency; and n is an integer number.

Tracking the occurrences of the SSC of varying screen angles, we found that the SSC are located on lines. All signal components in $\mathrm{SSC}_{\alpha\in\{1,2,3,\ldots\}}$ are kept on horizontal and vertical lines, or move along certain directions. This situation is shown in Fig. 14. Corresponding to the fact that the halftone angles range from 0° to 90°, the directions of the SSC movements ranges from -45° to 45°. Because negative halftone angles create symmetric moving paths, only 0°–45° angle changes are illustrated in Fig. 15. As we know, the SSC of higher frequencies are weaker, and generally, the elements in $\mathrm{SSC}_{\alpha>2}$ are too weak to generate significant moiré patterns. Therefore it is acceptable to analyze $\mathrm{SSC}_{\alpha\leqslant 2}$ only and to find an effective way for moiré suppression.

Fig. 15(a) illustrates the moving paths of the moiré signal sets for different screen angles, 0° to 45°, using the MCSR calculated by Eq. (18) with $n = 3$. Two cases are discussed here. One is for the angles in 0°–22.5° and the other is for the angles in 22.5°–45°. The SSC moving paths for these two cases are illustrated in Fig. 15(b) and Fig. 15(c),

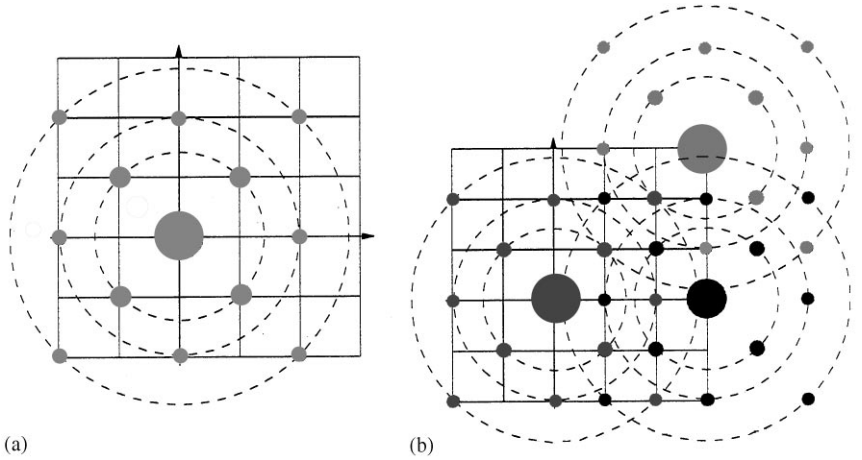

Fig. 13. Screen signal components (MCSR) of 45° screen. (a) The SSC of 45° halftone. (b) The SSC of 45° halftone on the image scanned by MCSR(45°).

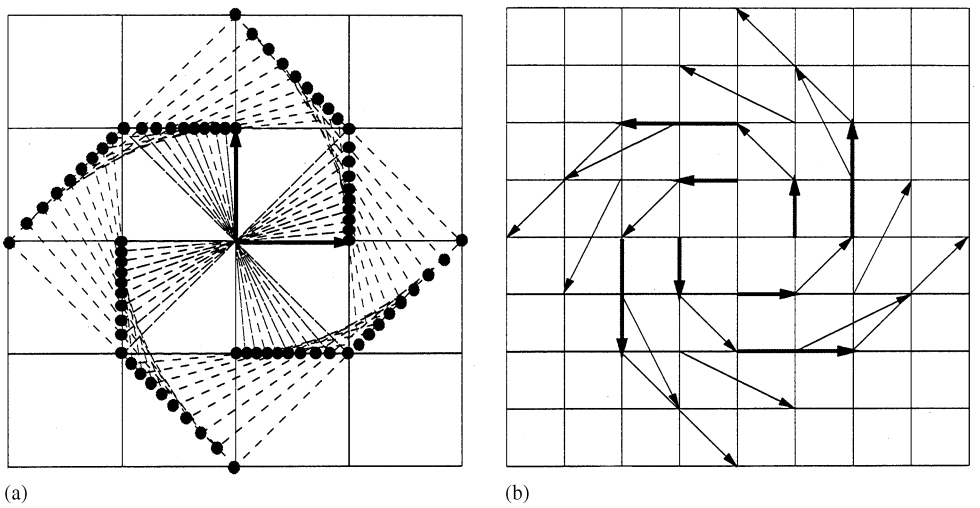

Fig. 14. Locations of SSC for any angled screen scans using the moiré controlling scanning resolution. (a) SSC_1 and $SSC_{\sqrt{2}}$ of 0°–45° screens. (b) SSC_1, $SSC_{\sqrt{2}}$, SSC_2, $SSC_{\sqrt{5}}$ and $SSC_{2\sqrt{2}}$ of 0°–45° screens.

respectively. The overlapping $SSC_{\alpha \leqslant 2}$ signals are illustrated in Fig. 15(d) and Fig. 15(e). The overlapping $SSC_{\alpha \leqslant 2}$ signals are confined in the shaded areas. This phenomenon is concluded in Fig. 16. When the halftone angles are in $-22.5° \sim 22.5°$, the MSS will be confined in the areas shown in Fig. 16(a). For the halftone angles out of $-22.5°$–$22.5°$, the MSS is confined in the areas shown in Fig. 16(b). Obviously, all the moiré signals are placed on band tracks of line segments. And this property is useful for moiré suppression as discussed in the following section.

3.2. Filters to suppress moiré signals

From the previous analysis, we know that after a halftone image is scanned by the MCSR, the

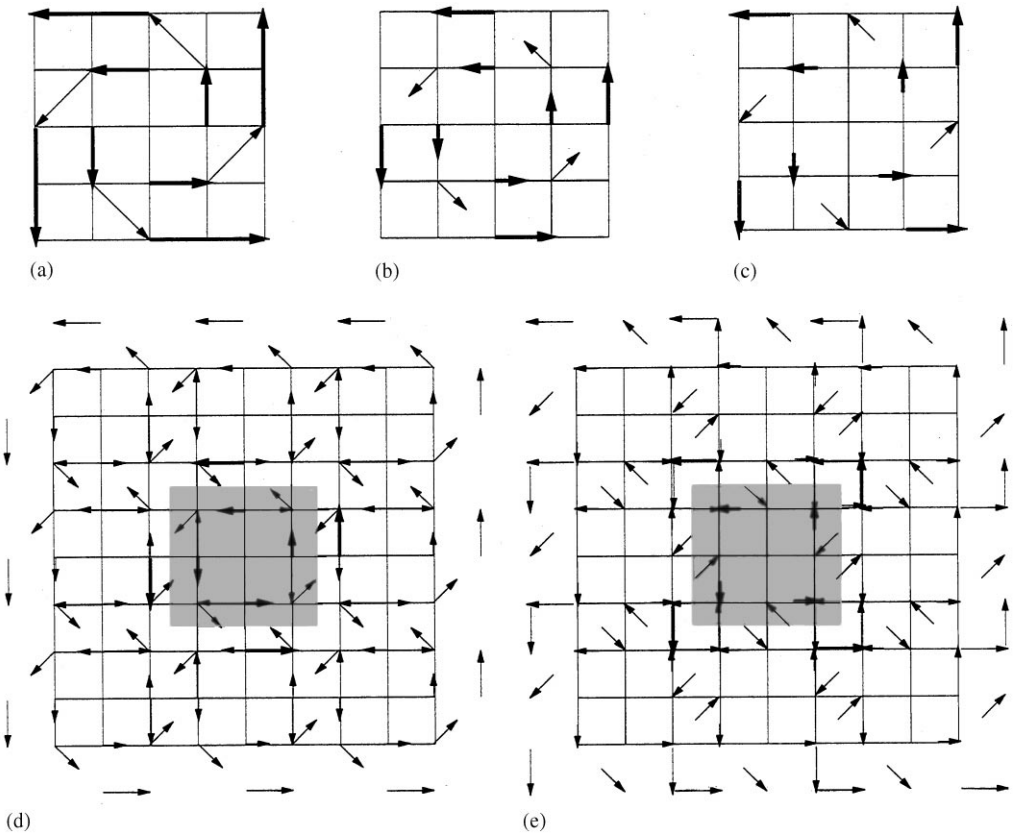

Fig. 15. The result of 0° to 45° screen scans using the MCSR with $n = 3$. (a) The SSC moving of 0°–45° halftone scanning using MCSR. (b) The SSC moving of 0°–22.5° halftone scanning using MCSR. (c) The SSC moving of 22.5°–45° halftone scanning using MCSR. (d) The result of 0°–22.5° screened halftone scanning using MCSR. (e) The result of 22.5°–45° screened halftone scanning using MCSR.

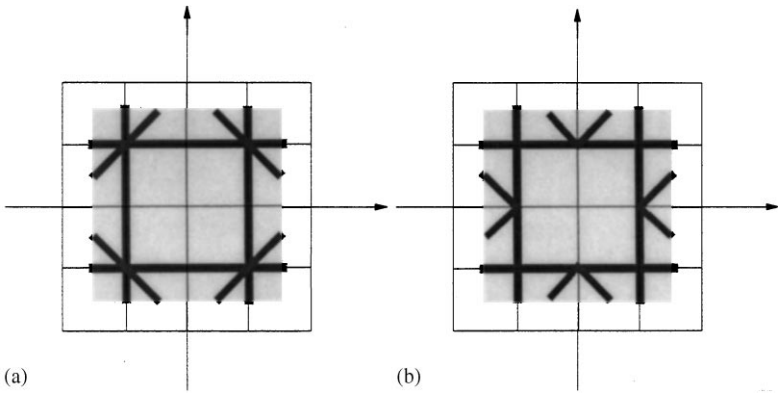

Fig. 16. The effect areas of the moiré signal components for $n = 3$. (a) $|\theta| \leqslant 22.5°$. (b) $22.5° < |\theta| \leqslant 45°$.

moiré signal sets are placed in known areas. By filtering out these signals, a better moiré suppressed image can be obtained. Certainly, we may erase these signals in the frequency domain by the FFT and the inverse FFT. However, due to processing time consideration, we prefer spatial operations to frequency operations. Some useful spatial filters for moiré suppression are proposed in the following.

The first useful spatial filter to suppress the moiré signal is the averaging filter. The averaging filter is defined as a convolution of the image intensity function and a rectangle function. The rectangle function is defined as

$$\mathrm{rect}(x, y) = \begin{cases} 1, & \text{where } |x| \leqslant a, |y| \leqslant a, \\ 0, & \text{elsewhere,} \end{cases}$$

where a is a positive value. The Fourier transform of the rectangle function is a two-dimensional sinc function:

$$\Im\{\mathrm{rect}(u, v)\} = \frac{\sin(2\pi a u)}{\pi u} \frac{\sin(2\pi a v)}{\pi v}.$$

The convolution of two functions in the spatial domain is equivalent to the multiplication in the frequency domain. When the value of the rectangle function in the frequency domain is zero, the signals of that frequency can be erased by convolution. Therefore, the averaging filter can be employed to clear or weaken signals in certain high-frequency areas. Fig. 17 shows two rectangle functions in the frequency domain. For a digital image, the equivalent averaging filter in the spatial domain is a constant pixel matrix. Fig. 18 shows the 2×2 and the

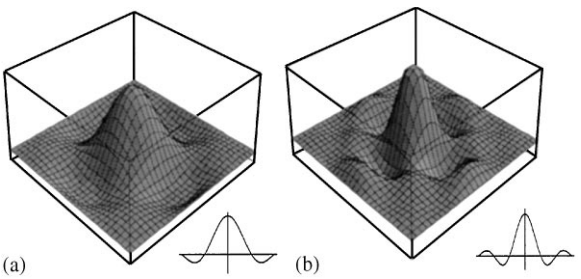

Fig. 17. Two averaging filters in the frequency domain. (a) $a = 2/2$. (b) $a = 3/2$.

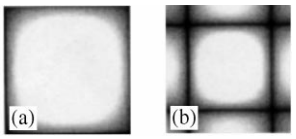

Fig. 18. The Fourier spectra of the digital averaging filters of Fig. 17 in the frequency domain. (a) 2×2. (b) 3×3.

3×3 digital averaging filters. The averaging filter clears four bands of signals in the frequency domain. According to Fig. 16, the moiré signal sets are connected as line segments. Since the connected line segments match the cleared bands, the averaging filter can be employed to suppress the moiré signals. For example, when the MCSR is calculated with $n = 3$, we can use the 3×3 averaging filter to suppress the moiré signals. Certainly, one may select bigger n values to calculate a higher MCSR for scanning. Practically, $n = 3$ is acceptable for most cases.

According to the discussion in the previous section, moiré signals are placed on the screening grid if the screen angle of the halftone is 0°, 45° or 90°. And the signals are easy to erase by the averaging filters. For the other screen angles, the SSC_1 is placed on the horizontal or vertical lines. The signals on the lines can also be easily erased by the averaging filter. After that, one or more filters are required to erase the remaining moiré signals that are generated by higher-ordered SSC. The averaging filters as well as a set of conceivable spatial filters that might be used to suppress moiré signals are listed in Fig. 19. Areas where moiré signals possibly exist for these cases can be determined by tracking the SSC. Then, a suitable filter to suppress the remaining moiré signals can be selected. And in this way a moiré suppression scanning procedure can be derived.

For example, for halftone images other than 45°, the MCSR can be calculated by (18). The $n \times n$ averaging filter then may be employed to suppress the major moiré patterns generated by SSC_1. After that, a filter listed in Fig. 19 is selected to suppress the remaining moiré signals. More specifically, we may first perform 3×3 averaging filtering, using the filter shown in Fig. 19(e), on an image that is scanned using the MCSR of $n = 3$. If the screen angle is

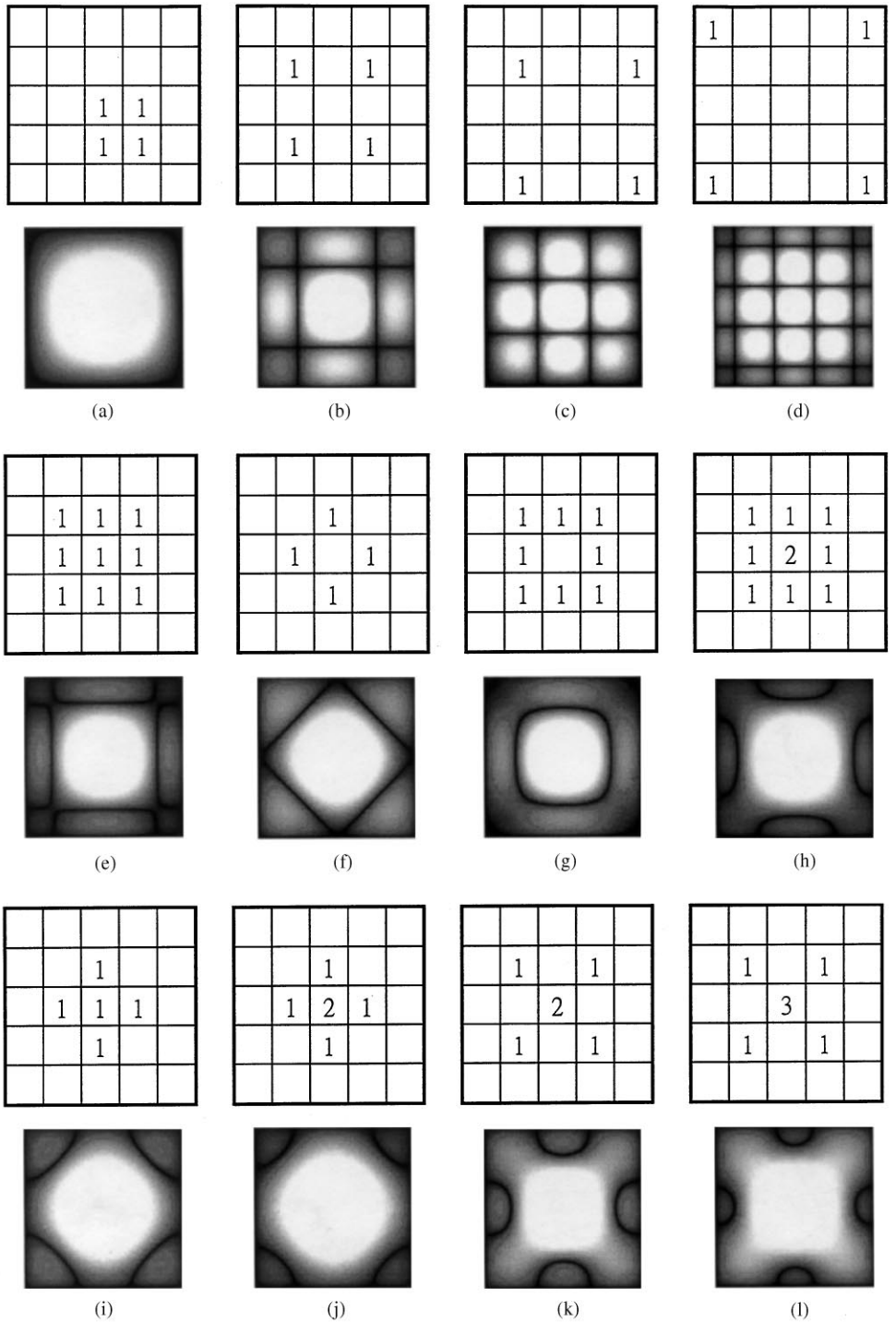

Fig. 19. Some useful spatial filters and their Fourier spectra.

between 22.5° and 67.5°, the moiré signals can be estimated by Fig. 16(a) and the filter shown in Fig. 19(k) can be used to suppress the remaining moiré patterns. Otherwise, the filter shown in Fig. 19(j) can be used.

3.3. Image normalization

For low-end scanners, the scanning resolution cannot be freely adjusted. Therefore, a normalization of the scanned image is necessary. For this case, moiré signals may not concentrate on lines. We propose here a procedure that may be used to adjust the scanning result to have a desired MCSR. Because the moiré signals are already generated by the first scan, only the major low-ordered moiré signal is considered to be suppressed.

First, scan the image using a resolution as high as possible in order to keep the generated moiré signals as weak as possible. Secondly, calculate a scaling ratio by the following formula:

$$\text{scaling ratio} = \frac{\text{desired MCSR}}{\text{current resolution}}. \tag{19}$$

Then, use the scaling ratio to re-sample the scanned image to generate a new image with the MCSR. Finally, follow the procedure proposed in the previous section to select a spatial filter to erase the moiré signals.

3.4. Digital screen tester

Accurate screen parameters, including the screen angle and the screen frequency, are required for the calculation of the MCSR. A digital screen tester is proposed here to measure the screen parameters by analyzing the Fourier spectrum of screened halftone images. Digital screen testing using the tester is a separate process from the moiré suppression process. One may perform the testing and keep the records of the resulting screen parameters for different types of document. The records may be used for future scanning to achieve moiré suppression.

According to the previous analysis of the screen signals, we know that, in the frequency domain, the screen signal components are placed on the reciprocal screening grid and can be classified by frequency. The most significant signals on the screening grid are the largest screen signal components, SSC_1. By checking the location of the spectrum signal peaks, the screen parameters can be determined. According to the symmetry property of the screen signals, the detection of the screen parameters may be simplified by expressing the spectrum in polar coordinates to yield a function $S(r, \theta)$, where S is the spectrum function, and r and θ are the variables in this coordinate system. Because the screen signal components are symmetric signal peaks, four significant signal peaks with 90° intervals can be found in the function $S(r, \theta)$. To detect these peaks, a function as follows is defined:

$$N(r,\theta) = \min\{S(r, \theta), S(r,\theta + 90^\circ), S(r, \theta + 180^\circ), S(r,\theta + 270^\circ)\},$$

where θ is an angle in the range of 0°–90°. Let $\hat{r}$ and $\hat{\theta}$ be the values such that

$$N(\hat{r}, \hat{\theta}) = \max_{r,\theta} N(r, \theta),$$

then $\hat{r}$ and $\hat{\theta}$ are taken to be the desired screen frequency and screen angle, respectively.

Practically, the detection of the screen parameters is designed in the following way. Firstly, a range of the possible screen frequency r is predetermined, normally from 50 LPI to 200 LPI. Then a pre-selected block of the screened halftone image is scanned by a high resolution (higher than a pre-determined largest frequency), and the scanning result is Fourier-transformed to yield a Fourier spectrum. Finally, in the pre-determined range of screen frequencies $50\ \text{LPI} \leqslant r \leqslant 200\ \text{LPI}$, the desired screen parameters, $\hat{r}$ and $\hat{\theta}$, can be determined. An example of the detection result is shown in Fig. 20.

3.5. Summary of proposed moiré suppression scanning procedure

A summary of the proposed moiré suppression scanning procedure described previously is given here. At the beginning, we measure the screen angle

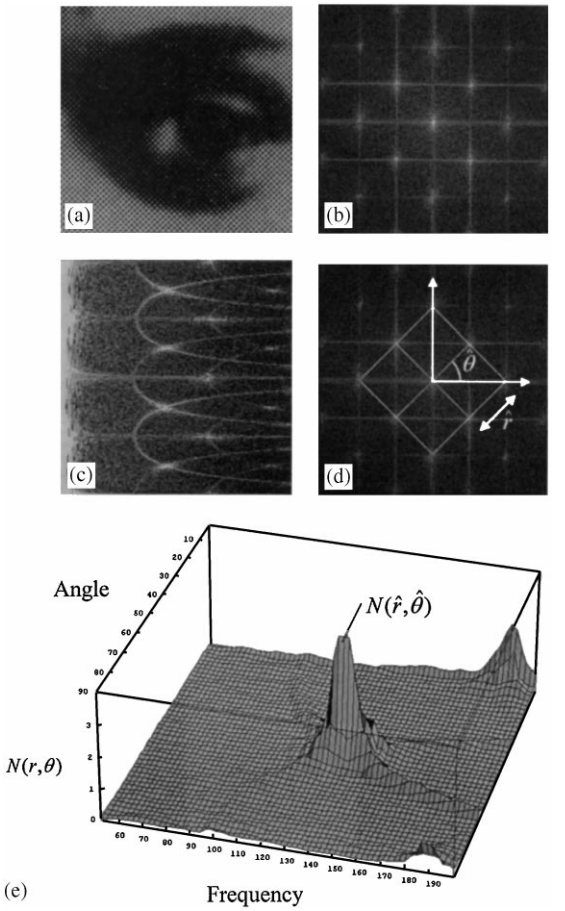

Fig. 20. Detection of the screen parameters. (a) Halftone image (600 DPI). (b) Fourier spectrum of (a). (c) $S(r, \theta)$. (d) Detection result. (e) $N(r, \theta)$.

and frequency of a given image by a screen tester. After that, depending on the scanner characters and the screen angles, three cases are treated.

Case 1. When the screen angle is 0°, 90° or 45° and the scanning resolution is freely adjustable, calculate the MCSR by Eq. (18) using any integer number n. Then, scan the halftone image using the MCSR. Finally, apply an $n \times n$ averaging filter to the scanning result and a moiré-suppressed image can be obtained.

Case 2. When the screen angle is different from 0°, 90° and 45° and the scanning resolution is freely adjustable, calculate the MCSR by Eq. (18) using any integer number n. Then, scan the halftone image using the MCSR. The moiré signals are now confined in certain areas in the frequency domain. Finally, use spatial filters in Fig. 19 to erase the moiré signals and yield a moiré-suppressed image. Here, $n = 3$ is recommended to calculate the MCSR. Then, use the averaging filter in Fig. 19(e), to suppress the major moiré signals, and apply the filter in Fig. 19(i) to erase the remaining moiré signals if the screen angle is in the range of $-22.5°$ to 22.5° For other screen angles, apply the filter in Fig. 19(k) to remove the remaining moiré signals.

Case 3. When the scanner resolution is fixed to some values that are different to the MCSR, a normalization process is necessary. First, scan the image using a resolution as high as possible. Then, resample the scanning result by the scaling ratio defined in Eq. (19). After this normalization, the procedure described in Case 1 and Case 2 can be employed to suppress the moiré signals.

4. Experimental results

Two types of experiment were conducted. In the first type we scanned one halftone image by a high-end drum scanner whose scanning resolution is freely adjustable. And in the second, another halftone image was scanned by a low-end handy scanner so that the process of normalization can be tested.

The first original halftone printing was printed using a 100 LPI and 45° screen. Firstly, we calculated the MCSR that is $3 \times \cos 45° \times$ screening resolution $= 3 \times \cos 45° \times 100 = 212$ DPI. After scanning with the MCSR, the image shown in Fig. 21 was obtained. By checking the Fourier spectrum, it is seen obvious that the moiré signals are placed on lines. Then, we performed a 3×3 averaging filtering on the image. The result is shown in Fig. 22. Clearly, the major moiré signals are suppressed. Finally, a sharpening filtering was performed to enhance the high-frequency signals. The resulting image is shown in Fig. 23. By checking the Fourier spectrum, most of the moiré signals are erased. The image is now ready to scale to any

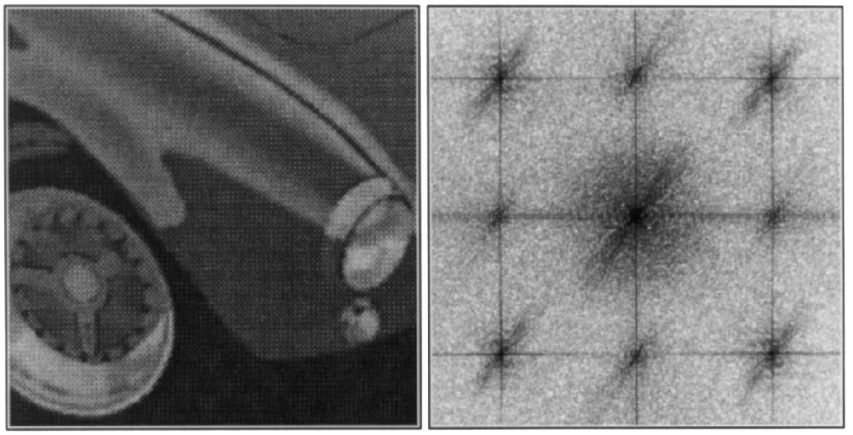

Fig. 21. A halftone image scanned by the MCSR.

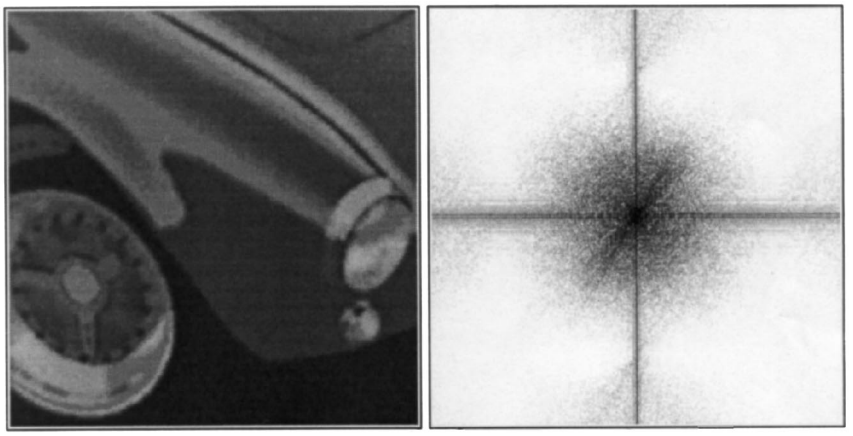

Fig. 22. Result of the 2×2 averaging filtering.

resolution for various usages, without producing significant moiré patterns. To check this, we scale the image down to 70 DPI, a resolution we know to cause obvious moiré patterns in usual cases. An additional scanning of the original printing using 70 DPI was performed for comparison. The two results are shown in Fig. 24. Obviously, the image produced by the proposed approach is much better than the one obtained from direct scanning which has a lot of moiré patterns.

The second experiment is more complicated. A handy scanner was used. The resolution of the scanner is fixed to 100, 150, 200, 300 and 400 DPI. The second printing scanned has 120 LPI screen frequency and 105° (15°) screen angled halftone. Initially, we use the highest available scanning resolution, 400 DPI, to scan the printing. Then, the image is scaled to $3 \times 120 \times \cos 15^\circ = 348$ DPI. Finally, a 3×3 averaging filter and the spatial filter in Fig. 16(k) were applied to the image. Fig. 25 shows the intermediate result for each stage. For comparison, we also scaled the result to 100 DPI and performed an additional scan using the same scanner. The two images are shown in Fig. 26. Obviously, the image produced by our approach is superior to that scanned by the traditional way.

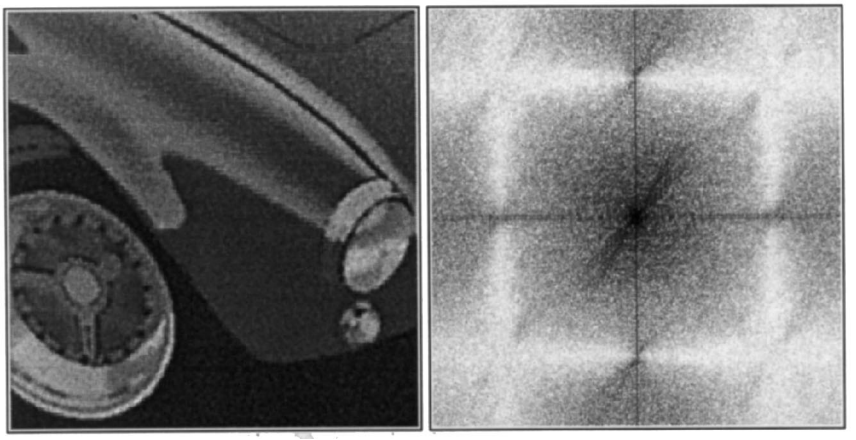

Fig. 23. Result of the sharpening.

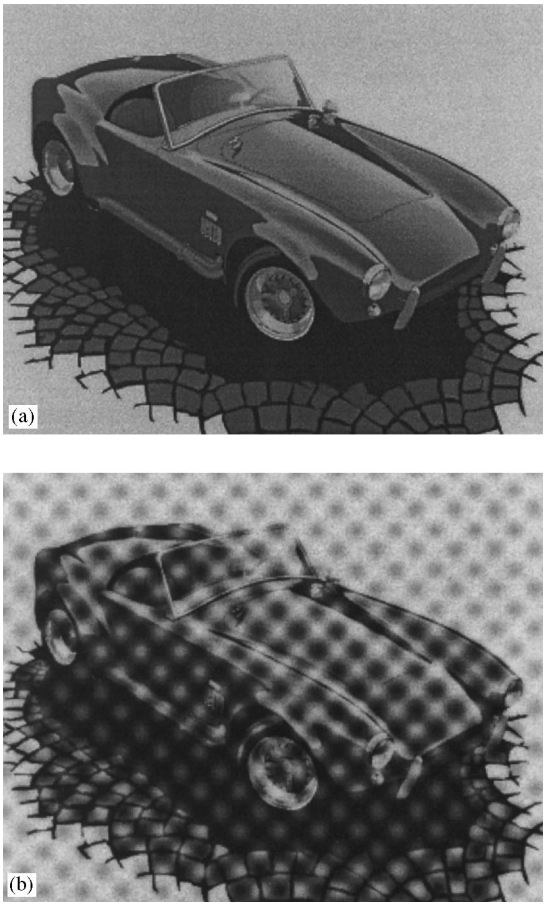

Fig. 24. A comparision between the results of proposed and the traditional scanning. (a) The result from the proposed method. (b) The result of traditional scanning.

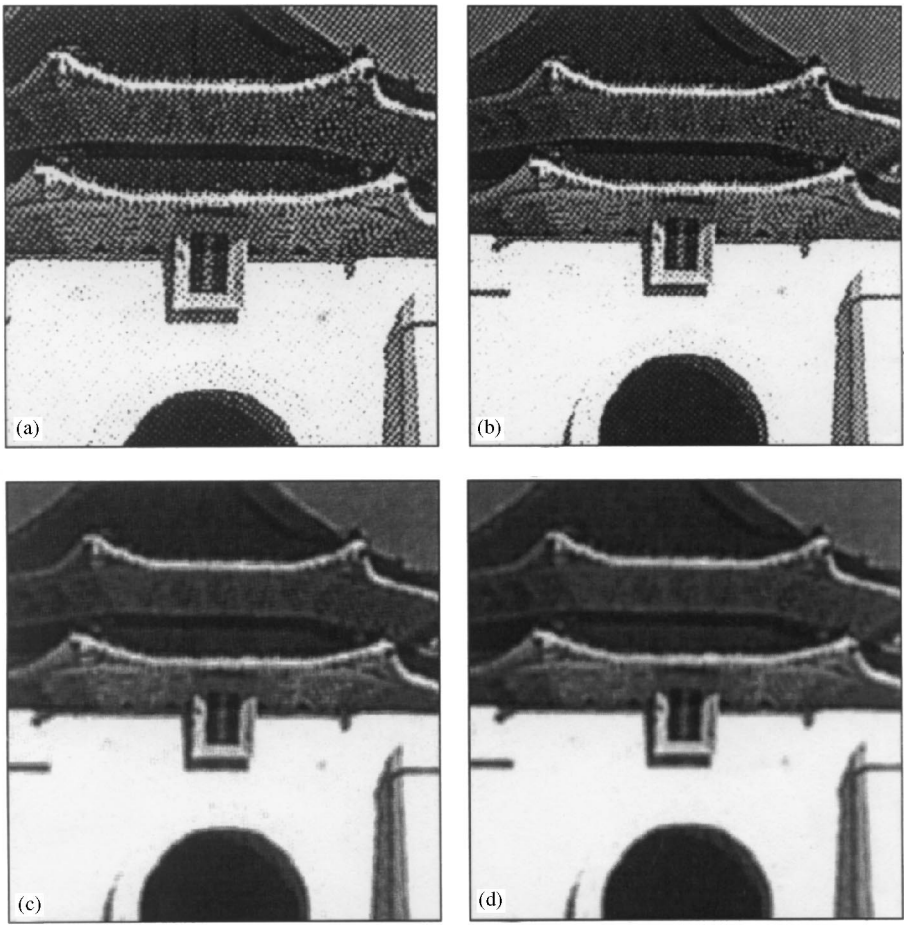

Fig. 25. Normalization and moiré suppression results for a halftone image scanned by a handy scanner. (a) Result of initial scanning (400 DPI). (b) Result of normalization (scale to 348 DPI). (c) Result of 3×3 averaging filtering. (d) Result of spatial filtering 16(k).

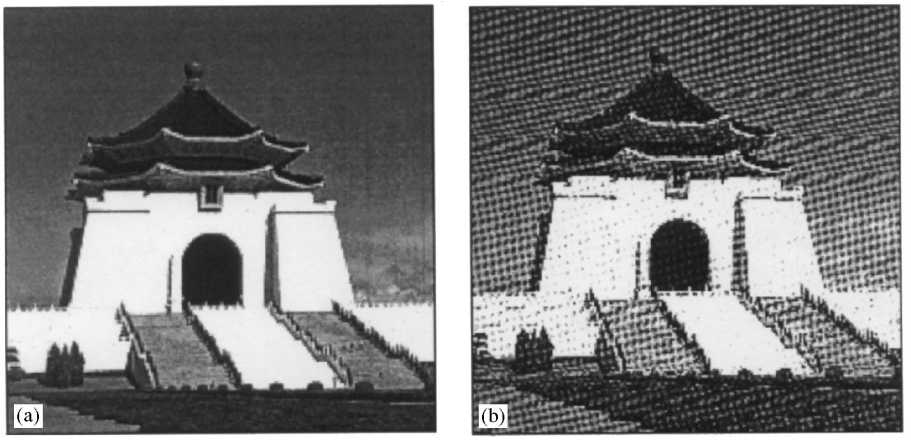

Fig. 26. A comparison between the results of traditional scanning. (a) The result from the proposed method. (b) The result of traditional scanning.

5. Conclusions

When scanning a halftone printing, additional moiré patterns will appear in the scanning result. By Fourier analysis, we have shown that these are aliasing patterns coming from the sampling of the screened halftone image by a scanner. A strategy has been proposed to design a scanning procedure that can suppress the additional moiré patterns. Firstly, we calculate an MCSR to keep the moiré signals in certain frequency domain areas. Then, we select specially-designed spatial filters to suppress the moiré signals. Because the redundant high-frequency moiré signals are suppressed, the resulting image is good for reproduction, image compression, and rescaling.

References

[1] I. Amidror, R.D. Hersch, V. Ostromoukhov, Spectral analysis and minimization of moiré patterns in color separation, Journal of Electronic Imaging 3 (3) (July 1994) 295–317.

[2] Z. Fan, Retrieval of gray images from digital halftones, in: IEEE Internat. Symposium on Circuits and Systems, San Diego CA, USA, 1992, pp. 2477–2480.

[3] Y. Fukuda, Analysis of superposed moiré patterns in halftone screen, Systems and Computers in Japan 21 (2) (1990) 105–111.

[4] C.M. Miceli, K.J. Parker, Inverse halftoning, Journal of Electronic Imaging 1 (2) (April 1992) 143–151.

[5] Y. Morimoto, Y. Seguchi, M. Okada, Screening and moiré suppression in printing and its analysis by Fourier transform, Systems and Computers in Japan 21 (2) (1990) 387–394.

[6] K. Patorski, Handbook of the Moiré Fringe Technique, Elsevier, Amsterdam, The Netherlands, 1993.

[7] P.G. Roetling, Halftone method with edge enhancement and moiré sppression, J. Opt. Soc. Amer. 66 (10) (October 1976) 985–989.

[8] A. Rosenfeld, A.C. Kak, Digital Picture Processing, 2nd edn., Vol. 1, Academic Press, New York, USA, 1982.

[9] J.C. Russ, The Image Processing Handbook, Boca Raton CRC Press, Florida, USA, 1993.

[10] S.P. Shu, C.L. Yeh, Moiré factors and visibility in scanned and printed halftone images, Optical Engineering 28 (7) (July 1989) 805–812.

[11] R. Ulichney, Digial Halftoning, MIT Press, Cambridge, 1987.